J. Fluid Mech. (1992), *vol.* 245, *pp.* 437–447

Low-speed two-dimensional free-surface flow past a body

By S. L. COLE AND T. D. STRAYER
Department of Mathematical Sciences, Rensselaer Polytechnic Institute, Troy, NY 12180-3590, USA

(Received 27 September 1991)

This paper defines the linearized problem of free-surface flow past a shallow two-dimensional body in terms of complex variables and provides an asymptotic solution for the Froude number tending to zero. The simple case of flow past a rectangular box with a triangular extension in front is worked out as an example. The low-Froude-number solution for 'double-body' flow in a fully infinite fluid past the same box with its reflection in the upper half-plane is also calculated. The upstream free-surface height for the linear solution is compared to the equivalent free-surface height for the double-body flow. Experimental results for this body are also presented and compared.

1. Motivation

Experiments were performed with a rectangular box towed in a tank 24.5 m long and 1.2 m wide with an average water depth of approximately 1.0 m. The box was submerged approximately 12 cm and had a clearance of approximately 4 cm between the box ends and the tank wall. The 4 cm clearance allowed surface contaminants to drain around the edges. Waves generated upstream of the towed box were nearly two-dimensional except close to the sidewalls. Wave profiles were measured using a capacitance type wave gauge positioned at the midpoint of the tank to avoid interference with reflected waves and to avoid surface contaminants that tended to build up near the endwalls. It was observed experimentally that the potential flow upstream of the towed box separated away from the free surface, passing under and driving a nearly triangular-shaped vortical flow region as depicted in figure 1. (A more complete description of the experimental set-up and a simple model and numerical calculation of the flow in the vortical region is given in Cole & Strayer 1991.) Unsteady waves were shed from the bow. However, for moderately high Froude numbers these waves were attenuated in the vortical flow region and the upstream potential flow appeared very similar to the double-body flow past an infinite box with a triangular extension in front from a few draught lengths out in front of the box. Double-body flow does not predict downstream waves or their accompanying drag. Yet, downstream waves exist. It was conjectured that the potential flow could perhaps be modelled as a solution to the linearized problem of flow past a shallow box with a triangular extension in front since linearized theory predicts waves downstream. Does it also mimic the double-body upstream for small Froude number? The purpose of this paper is to address this question.

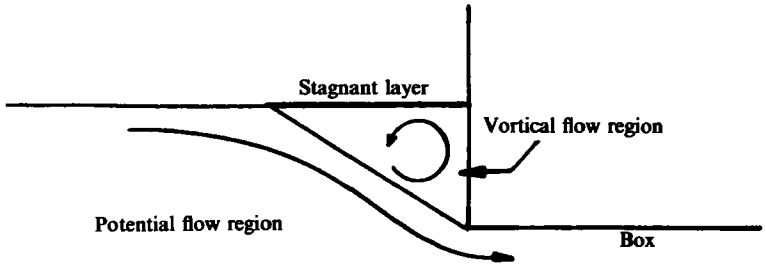

FIGURE 1. Observed free-surface flow past a towed rectangular box.

2. Problem formulation

The two-dimensional equations of potential flow past an object in dimensional variables are

$$\left.\begin{aligned} \Phi^*_{x^*x^*}+\Phi^*_{z^*z^*}&=0,\\ \Phi^*_{z^*}=\Phi^*_{x^*}\xi^*_{x^*} \quad &\text{on} \quad z^*=\xi^*(x^*),\\ P^*/\rho^*+\tfrac{1}{2}(\Phi^{*2}_{x^*}+\Phi^{*2}_{z^*})+g^*z^*=\tfrac{1}{2}U^{*2} \quad &\text{on} \quad z^*=\xi^*(x^*), \end{aligned}\right\} \tag{1}$$

where Φ^* is the velocity potential, P^* is the pressure taken to be zero along the free surface, ρ^* is the density, g^* is the gravitational acceleration, ξ^* is the surface height with $z^*=\xi^*=d^*f$ along the body and where d^* is the draught and f is the body shape. The coordinate frame is fixed relative to the body so there is a uniform flow with velocity, U^*, heading toward the object from upstream infinity. Φ^*, ξ^* and their derivatives are assumed to decay as x^* tends to upstream infinity or z^* tends to negative infinity. The body has length $2L^*$.

In order to solve the linear approximation based on the assumption that the body's draught is much smaller than its length, (1) are cast in non-dimensional form by scaling according to the half-length, L^*, and the velocity, U^*. Substituting

$$\Phi=\frac{\Phi^*}{U^*L^*}, \quad x=\frac{x^*}{L^*}, \quad z=\frac{z^*}{L^*}, \quad \xi=\frac{\xi^*}{L^*}, \quad \epsilon f=\frac{d^*f}{L^*}, \quad P=\frac{P^*}{\rho^*g^*L^*} \tag{2}$$

into (1) gives

$$\left.\begin{aligned} \Phi_{xx}+\Phi_{zz}&=0,\\ \Phi_z=\Phi_x\xi_x \quad &\text{on} \quad z=\xi,\\ P+\tfrac{1}{2}F_L^2(\Phi_x^2+\Phi_z^2)+z=\tfrac{1}{2}F_L^2 \quad &\text{on} \quad z=\xi, \end{aligned}\right\} \tag{3}$$

where $\xi=\epsilon f$ on the body. The non-dimensional parameters are $\epsilon=d^*/L^*$, a measure of the shallowness of the body, and F_L, the Froude number based on the half-length of the body; $F_L^2=U^{*2}/(g^*L^*)$.

Since linear theory is based on the assumption that the body's draught is much smaller than its length, ϵ is assumed to be much smaller than 1 and (3) can be linearized using the perturbation expansions

$$\left.\begin{aligned} \Phi(x,z;\epsilon,F_L)&=x+\epsilon\phi(x,z;F_L)+\ldots,\\ \xi(x;\epsilon,F_L)&=\epsilon\eta(x;F_L)+\ldots,\\ P(x,\xi;\epsilon,F_L)&=\epsilon p(x;F_L)+\ldots, \end{aligned}\right\} \tag{4}$$

to give

$$\phi_{xx}+\phi_{zz}=0, \tag{5a}$$

$$\phi_z=\eta_x \quad \text{on} \quad z=0, \tag{5b}$$

$$p+F_L^2\phi_x+\eta=0 \quad \text{on} \quad z=0, \tag{5c}$$

with $\eta = f$ along the body and ϕ, η and their derivatives tending to zero as x tends to upstream infinity or z tends to negative infinity. Equations (5) are the linearized equations for potential flow past a shallow object. This is a mixed boundary-value problem where the flow is tangent to the body along the object but satisfies free-surface conditions off the body. Thus, even though (5) define a linear problem, they are difficult to solve for arbitrary values of F_L.

We wish to compare the linear and experimental results with the double-body solution for a finite and a semi-infinite body and, therefore, scale (1) to define the double-body problem using the draught, d^*, and the velocity, U^*. Substituting

$$\tilde{\Phi} = \frac{\Phi^*}{U^* d^*}, \quad \tilde{x} = \frac{x^*}{d^*}, \quad \tilde{z} = \frac{z^*}{d^*}, \quad \tilde{\xi} = \frac{\xi^*}{d^*}, \quad \tilde{P} = \frac{P^*}{\rho^* g^* d^*} \tag{6}$$

into (1) gives

$$\left.\begin{aligned} \tilde{\Phi}_{\tilde{x}\tilde{x}} + \tilde{\Phi}_{\tilde{z}\tilde{z}} &= 0, \\ \tilde{\Phi}_{\tilde{z}} = \tilde{\Phi}_{\tilde{x}} \tilde{\xi}_{\tilde{x}} \quad &\text{on} \quad \tilde{z} = \tilde{\xi}, \\ \tilde{P} + \tfrac{1}{2} F_d^2 (\tilde{\Phi}_{\tilde{x}}^2 + \tilde{\Phi}_{\tilde{z}}^2) + \tilde{z} = \tfrac{1}{2} F_d^2 \quad &\text{on} \quad \tilde{z} = \tilde{\xi}, \end{aligned}\right\} \tag{7}$$

with $\tilde{\xi} = f$ along the body and where F_d is the Froude number based on the draught of the body; $F_d^2 = U^{*2}/(g^* d^*)$. Note that $\tilde{\Phi}$ depends on the parameter $1/\epsilon$ since the length of the body has been scaled by d^*.

In the double-body approximation, F_d is assumed to be much smaller than 1 and the parameter $1/\epsilon$ is assumed to be of order 1. Then (7) can be simplified using the perturbation expansions

$$\left.\begin{aligned} \tilde{\Phi}(\tilde{x}, \tilde{z}; F_d, 1/\epsilon) &= \tilde{\phi}(\tilde{x}, \tilde{z}; 1/\epsilon) + \ldots, \\ \tilde{\xi}(\tilde{x}; F_d, 1/\epsilon) &= F_d^2 \tilde{\eta}(\tilde{x}; 1/\epsilon) + \ldots \end{aligned}\right\} \tag{8}$$

to yield

$$\left.\begin{aligned} \tilde{\phi}_{\tilde{x}\tilde{x}} + \tilde{\phi}_{\tilde{z}\tilde{z}} &= 0, \\ \tilde{\phi}_{\tilde{z}} = 0 \quad &\text{on} \quad \tilde{z} = 0 \quad \text{and} \quad \tilde{x} \text{ off the body}, \\ \tilde{\phi}_{\tilde{z}} = \tilde{\phi}_{\tilde{x}} f_{\tilde{x}} \quad &\text{on} \quad \tilde{z} = f \quad \text{and} \quad \tilde{x} \text{ on the body}, \\ \tilde{\eta} = \tfrac{1}{2}[1 - \tilde{\phi}_{\tilde{x}}^2] \quad &\text{on} \quad \tilde{z} = 0 \quad \text{and} \quad \tilde{x} \text{ off the body}, \end{aligned}\right\} \tag{9}$$

where $\tilde{\phi}, \tilde{\eta}$ and their derivatives tend to zero as $\tilde{x}$ tends to upstream infinity or $\tilde{z}$ tends to negative infinity. Equations (9) are the double-body equations for low-Froude-number potential flow. Note that these equations are also linear; however, they are substantially simpler to solve than the shallow-draught problem as (9) do not represent a mixed boundary-value problem. We wish to compare the solution of the linearized problem, (5), in the limit as F_L tends to zero with the solution of the double-body problem, (9), in the limit as the draught-to-length ratio, ϵ, tends to zero.

3. Linear problem

Following ideas similar to those of Keldysh (1939) and Sedov (1965) for two-dimensional planing theory, the linear problem can be recast in terms of complex variables as follows. Let ϕ be the real part of an analytic function G of the complex variable $\zeta = x + iz$. Then ϕ automatically satisfies Laplace's equation. Following the ideas of Cole (1988) for three-dimensional flat-ship theory, let $p(x)$ be the real part of the analytic function Π evaluated at $z = 0$. Differentiating (5*c*) with respect to x and substituting (5*b*) implies the surface terms of the linear problem, (5), are equivalent to

$$\mathrm{Re}\{\Pi_\zeta + F_L^2 G_{\zeta\zeta} + iG_\zeta\} = 0 \quad \text{on} \quad z = 0 \tag{10a}$$

with $$\operatorname{Im} G_\zeta = -f_x \quad \text{for} \quad z = 0 \quad \text{and} \quad x \text{ on the body.} \tag{10b}$$

Equation (10a) can be integrated once to yield

$$\operatorname{Re}\{\Pi + F_L^2 G_\zeta + \mathrm{i}G\} = 0 \quad \text{on} \quad z = 0 \tag{11a}$$

since $p = 0$ on the free surface and ϕ and its derivatives tend to zero as ζ tends to upstream infinity. Equation (10b) is equivalent to

$$\operatorname{Im} G = -f \quad \text{on the body.} \tag{11b}$$

The solution of problem (11) can be motivated as follows. Equation (11a) will be satisfied if Π and G satisfy

$$\Pi + F_L^2 G_\zeta + \mathrm{i}G = 0 \tag{12}$$

everywhere. We are free to choose a series solution for either G or Π and solve (12) for the other function. The series solutions, however, must ensure that $\operatorname{Re}\{\Pi\} = 0$ on $z = 0$ off the body and that $F_L^2 G_\zeta + \mathrm{i}G$ satisfies the correct decay behaviour as ζ tends to infinity. This can be done by a judicious choice for Π. There are two cases in which (11) can be solved easily, $F_L^2 \gg 1$ and $F_L^2 \ll 1$.

3.1. *The case* $F_L^2 \gg 1$

The high-Froude-number case, $F_L^2 \gg 1$, is presented here because it serves as a model for the solution of the low-Froude-number case and because important differences arise between the two. The high-Froude-number case was solved by Sedov (1965) using numerical methods. In a very similar way, an asymptotic solution can be found for a body centred about $x = 0$ by expanding Π as

$$\Pi = \mathrm{i} \sum_{n=0}^{\infty} \frac{a_n (\zeta - (\zeta^2 - 1)^{\frac{1}{2}})^n}{(\zeta^2 - 1)^{\frac{1}{2}}} \tag{13}$$

for the constants, a_n, real and the branch cut chosen so that Π tends to zero as ζ tends to infinity. This implies $p = \operatorname{Re} \Pi = 0$ for $z = 0$ and $|x| > 1$ and that $F_L^2 G_\zeta + \mathrm{i}G = -\Pi$ has the correct decay behaviour as ζ tends to infinity as argued in Sedov (1965). Then, from (12)

$$F_L^2 G_\zeta + \mathrm{i}G = -\mathrm{i} \sum_{n=0}^{\infty} \frac{a_n (\zeta - (\zeta^2 - 1)^{\frac{1}{2}})^n}{(\zeta^2 - 1)^{\frac{1}{2}}}. \tag{14}$$

This is just an ordinary differential equation in ζ which can be solved to yield

$$G = -\frac{\mathrm{i}}{F_L^2} \mathrm{e}^{-\mathrm{i}\zeta/F_L^2} \int_{-\infty}^{\zeta} \mathrm{e}^{\mathrm{i}t/F_L^2} \sum_{n=0}^{\infty} a_n \frac{(t - (t^2 - 1)^{\frac{1}{2}})^n}{(t^2 - 1)^{\frac{1}{2}}} \mathrm{d}t. \tag{15}$$

An integration by parts of (15) shows that for $F_L^2 \gg 1$

$$G_\zeta \sim -\frac{\mathrm{i}}{F_L^2} \sum_{n=0}^{\infty} a_n \frac{(\zeta - (\zeta^2 - 1)^{\frac{1}{2}})^n}{(\zeta^2 - 1)^{\frac{1}{2}}}. \tag{16}$$

A Fourier series representation can be obtained by substituting $\zeta = x = \cos\theta$, along the body with $(\zeta^2 - 1)^{\frac{1}{2}} = -\mathrm{i}\sin\theta$, into (16) to yield

$$\operatorname{Im} G_\zeta \underset{\substack{F_L^2 \to \infty \\ \zeta \text{ on body}}}{\sim} -\frac{\mathrm{i}}{F_L^2} \sum_{n=1}^{\infty} a_n \frac{\sin n\theta}{-\mathrm{i}\sin\theta}. \tag{17}$$

Expanding $f_x = \sum_{m=0}^{\infty} b_m \cos m\theta$ and setting $\operatorname{Im} G_\zeta = -f_x$ from (10b) on the body yields

$$-F_L^2 \sum_{m=0}^{\infty} b_m \cos m\theta \sin\theta = \sum_{n=1}^{\infty} a_n \sin n\theta, \tag{18}$$

which defines the a_n for $n = 1, 2, \ldots$. The solution for G is not unique, however, until a_0 is specified. Sedov imposes the boundary condition that the high-speed flow leaves the trailing edge smoothly. Thus the free constant a_0 must be chosen so that $\Sigma_{n=0}^{\infty} a_n = 0$. This ensures that there is no singularity along the trailing edge. This leading-order problem is the same as that of lifting two-dimensional wing theory. The interpretation of the solutions is different, however. The identical solution in the semi-infinite fluid case of ship wave theory produces a spray drag at the leading edge (see Cole 1988) while in the fully infinite-fluid case of thin-wing theory, it produces a leading-edge thrust (see Jones 1990).

The method just presented can be continued relatively easily to calculate the next term in an asymptotic expansion for ϕ as F_L^2 tends to infinity. It will not be done here, however, as it is necessary only to understand the behaviour of the first term when we consider the low-Froude-number limit.

3.2. *The case* $F_L^2 \ll 1$

The solution for the low-Froude-number case cannot be found using (13) for Π as will be explained below but can be constructed instead from the expansion

$$\Pi = \mathrm{i} \sum_{n=1}^{\infty} a_n (\zeta - (\zeta^2 - 1)^{\frac{1}{2}})^n. \tag{19}$$

Equation (12) then implies

$$F_L^2 G_\zeta + \mathrm{i}G = -\mathrm{i} \sum_{n=1}^{\infty} a_n (\zeta - (\zeta^2 - 1)^{\frac{1}{2}})^n, \tag{20}$$

which can be solved to yield

$$G = -\frac{\mathrm{i}}{F_L^2} \mathrm{e}^{-\mathrm{i}\zeta/F_L^2} \int_{-\infty}^{\zeta} \mathrm{e}^{\mathrm{i}t/F_L^2} \sum_{n=1}^{\infty} a_n (t - (t^2 - 1)^{\frac{1}{2}})^n \, \mathrm{d}t. \tag{21}$$

On the free surface the real parts of the terms $F_L^2 G_\zeta$ and $\mathrm{i}G$ must be the same size since they sum to zero. On the body, however, derivatives of G are not expected to be large (except possibly near the leading or trailing edges). Thus, on the body $F_L^2 G_\zeta \ll \mathrm{i}G$ and (20) implies

$$\operatorname{Im} G|_{\substack{z=0 \\ |x|<1}} \sim \operatorname{Re}\left\{ \mathrm{i} \sum_{n=1}^{\infty} a_n (\zeta - (\zeta^2 - 1)^{\frac{1}{2}})^n \right\}_{F_L^2 \to 0}. \tag{22}$$

Substituting $\zeta = x = \cos\theta$ on $z = 0$ for $|x| < 1$ into (12*b*) and (22) yields

$$\sum_{n=1}^{\infty} a_n \sin n\theta \sim f(\theta) = \sum_{n=1}^{\infty} f_n \sin n\theta, \tag{23}$$

which determines all of the a_n uniquely once f is expanded in a sine series in θ. Note that unlike the high-speed theory, there is no free constant available to enable the flow solution to leave the trailing edge smoothly. Thus, the boundary conditions for the low- and high-Froude-number cases are different. Unlike high-Froude-number theory, the leading-order problem for the low-Froude-number case in ship wave theory does not correspond to any simple two-dimensional airfoil problem. The assumption that $F_L^2 G_\zeta \ll \mathrm{i}G$ on the body but away from $\zeta^2 = 1$ is easily verified from (21) and (23). It is now apparent why an expansion for Π of the form (13) could not be used in the low-Froude-number case. From (12) we see that the form of Π defines the singular behaviour of G_ζ for the high-Froude-number case and G for the low-

Froude-number case. In order for G_ζ to have at most a square-root singularity at the body's edges, Π cannot have an expansion of the form (13) in the low-Froude-number case since that would give rise to a solution for G and thus G_ζ when G is differentiated, which is too singular.

Equations (21) and (23) define a remarkably simple solution for the leading-order term in the low-Froude-number case. Unlike the high-speed case though, it is not easy to generate the next term in an asymptotic expansion for the low-speed solution. Some general comments about the behaviour of the low-Froude-number solution are made next.

Differentiation of (21) gives

$$G_\zeta = -\frac{\mathrm{i}}{F_L^2}\sum_{n=1}^{\infty} a_n(\zeta-(\zeta^2-1)^{\frac{1}{2}})^n - \frac{\mathrm{e}^{-\mathrm{i}\zeta/F_L^2}}{F_L^4}\int_{-\infty}^{\zeta}\mathrm{e}^{\mathrm{i}t/F_L^2}\sum_{n=1}^{\infty} a_n(t-(t^2-1)^{\frac{1}{2}})^n\,\mathrm{d}t$$

$$= \frac{\mathrm{e}^{-\mathrm{i}\zeta/F_L^2}}{\mathrm{i}F_L^2}\int_{-\infty}^{\zeta}\mathrm{e}^{\mathrm{i}t/F_L^2}\sum_{n=1}^{\infty}(-n)\,a_n\frac{(t-(t^2-1)^{\frac{1}{2}})^n}{(t^2-1)^{\frac{1}{2}}}\,\mathrm{d}t. \tag{24}$$

An integration by parts of (24) for $\zeta = x < -1$ yields

$$G_\zeta = \frac{1}{\mathrm{i}F_L^2}\mathrm{e}^{-\mathrm{i}\zeta/F_L^2}\int_{-\infty}^{\zeta}\mathrm{e}^{\mathrm{i}t/F_L^2}\sum_{n=1}^{\infty}(-n)\,a_n\frac{(t-(t^2-1)^{\frac{1}{2}})^n}{(t^2-1)^{\frac{1}{2}}}\,\mathrm{d}t$$

$$\underset{\zeta=x<-1}{=}\sum_{n=1}^{\infty} na_n\frac{(\zeta-(\zeta^2-1)^{\frac{1}{2}})^n}{(\zeta^2-1)^{\frac{1}{2}}} + \mathrm{e}^{-\mathrm{i}\zeta/F_L^2}\int_{-\infty}^{\zeta}\mathrm{e}^{\mathrm{i}t/F_L^2}\sum_{n=1}^{\infty}(-n)\,a_n\frac{\mathrm{d}}{\mathrm{d}t}\left[\frac{(t-(t^2-1)^{\frac{1}{2}})^n}{(t^2-1)^{\frac{1}{2}}}\right]\mathrm{d}t$$

$$\underset{\substack{F_L^2\to 0\\ \zeta=x<-1}}{\sim}\sum_{n=1}^{\infty} na_n\frac{(\zeta-(\zeta^2-1)^{\frac{1}{2}})^n}{(\zeta^2-1)^{\frac{1}{2}}}. \tag{25}$$

Thus, to leading order $\xi = \epsilon\eta = -\epsilon F_L^2\phi_x$ has no high-frequency waves upstream in the linear theory and the free-surface height depends on the Froude number only as a scale factor. Equation (25) is entirely real for $z = 0$ upstream of the body, thus $\phi_x \gg \phi_z$ on the surface. These properties are also true for double-body flow.

For $\zeta = x > -1$ consider the integral

$$I = \int_{-\infty}^{\zeta}\mathrm{e}^{\mathrm{i}t/F_L^2}\frac{(t-(t^2-1)^{\frac{1}{2}})^n}{(t^2-1)^{\frac{1}{2}}}\,\mathrm{d}t \tag{26}$$

from (24). For $\zeta = x$ for $|x| < 1$, the integral I can be rewritten as

$$I = \int_{-\infty}^{-1}\mathrm{e}^{\mathrm{i}t/F_L^2}\frac{(t-(t^2-1)^{\frac{1}{2}})^n}{(t^2-1)^{\frac{1}{2}}}\,\mathrm{d}t + \int_{-1}^{\zeta}\mathrm{e}^{\mathrm{i}t/F_L^2}\frac{(t-(t^2-1)^{\frac{1}{2}})^n}{(t^2-1)^{\frac{1}{2}}}\,\mathrm{d}t. \tag{27}$$

The first integral in (27) is

$$\int_{-\infty}^{-1}\mathrm{e}^{\mathrm{i}t/F_L^2}\frac{(t-(t^2-1)^{\frac{1}{2}})^n}{(t^2-1)^{\frac{1}{2}}}\,\mathrm{d}t = \int_{t\,\underset{-1^-}{\mathrm{near}}}\mathrm{e}^{\mathrm{i}t/F_L^2}\frac{(-1)^n}{(t^2-1)^{\frac{1}{2}}}\,\mathrm{d}t + O(F_L^2)$$

$$= F_L(-1)^n(\tfrac{1}{2}\pi)^{\frac{1}{2}}\mathrm{e}^{-\mathrm{i}(\pi/4+1/F_L^2)} + O(F_L^2). \tag{28}$$

The second integral in (27) is

$$\int_{-1}^{\zeta}\mathrm{e}^{\mathrm{i}t/F_L^2}\frac{(t-(t^2-1)^{\frac{1}{2}})^n}{(t^2-1)^{\frac{1}{2}}}\,\mathrm{d}t = \int_{t\,\underset{-1^+}{\mathrm{near}}}\mathrm{e}^{\mathrm{i}t/F_L^2}\frac{(-1)^n}{(t^2-1)^{\frac{1}{2}}}\,\mathrm{d}t + O(F_L^2)$$

$$= -F_L(-1)^n(\tfrac{1}{2}\pi)^{\frac{1}{2}}\mathrm{e}^{-\mathrm{i}(\pi/4+1/F_L^2)} + O(F_L^2). \tag{29}$$

Thus,

$$I \underset{\substack{F_L^2 \to 0 \\ \zeta = x, |x|<1}}{\sim} O(F_L^2) \tag{30}$$

and $\xi_x = \epsilon\eta_x = \epsilon f_x = \epsilon\phi_z$ is an order-ϵ quantity along the body as is expected. For $x > 1$,

$$I = \int_{-\infty}^{1} e^{it/F_L^2} \frac{(t-(t^2-1)^{\frac{1}{2}})^n}{(t^2-1)^{\frac{1}{2}}} dt + \int_{1}^{\zeta} e^{it/F_L^2} \frac{(t-(t^2-1)^{\frac{1}{2}})^n}{(t^2-1)^{\frac{1}{2}}} dt. \tag{31}$$

The first integral in (31) is

$$\int_{-\infty}^{1} e^{it/F_L^2} \frac{(t-(t^2-1)^{\frac{1}{2}})^n}{(t^2-1)^{\frac{1}{2}}} dt = \int_{t \underset{1^-}{\text{near}}} e^{it/F_L^2} \frac{(1)^n}{(t^2-1)^{\frac{1}{2}}} dt + O(F_L^2)$$

$$= F_L(\tfrac{1}{2}\pi)^{\frac{1}{2}} e^{i(\pi/4+1/F_L^2)} + O(F_L^2). \tag{32}$$

The second integral in (31) is

$$\int_{1}^{\zeta} e^{it/F_L^2} \frac{(t-(t^2-1)^{\frac{1}{2}})^n}{(t^2-1)^{\frac{1}{2}}} dt = \int_{t \underset{1^+}{\text{near}}} e^{it/F_L^2} \frac{(1)^n}{(t^2-1)^{\frac{1}{2}}} dt + O(F_L^2)$$

$$= F_L(\tfrac{1}{2}\pi)^{\frac{1}{2}} e^{i(\pi/4+1/F_L^2)} + O(F_L^2). \tag{33}$$

This gives

$$I \underset{\substack{x>1 \\ F_L \to 0}}{\sim} F_L(2\pi)^{\frac{1}{2}} e^{i(\pi/4+1/F_L^2)}. \tag{34}$$

Thus, $\xi = \epsilon\eta = -\epsilon F_L^2 \phi_x$ is order (ϵF_L) behind the body. Downstream of the body, the dominant term is a free wave of the form

$$\eta \underset{\substack{F_L \to 0 \\ x>1}}{\sim} -F_L(2\pi)^{\frac{1}{2}} \sum_{n=1}^{\infty} n a_n \sin[(x-1)/F_L^2 - \tfrac{1}{4}\pi] \tag{35}$$

with correction terms to this simple sine wave of order F_L^2.

4. Simple example

The linear and double-body solutions for flow past a box with a triangular extension in front as shown in figure 2 is worked out next. α is chosen to be $\alpha = \tan^{-1}(1/1.6)$ to agree with experimental observations for the geometry of the triangular-shaped vortical flow region in front of the towed rectangular box.

In this example,

$$f(x) = \begin{cases} \dfrac{-1}{1.6}(1+x) & \text{for} \quad -1 \leqslant x \leqslant -0.5 \\ \dfrac{-1}{1.6}(0.5) & \text{for} \quad -0.5 \leqslant x \leqslant 1. \end{cases} \tag{36}$$

Substituting $x = \cos\theta$ for $-\pi \leqslant \theta \leqslant 0$ gives

$$f(\theta) = \begin{cases} \dfrac{-1}{1.6}(1+\cos\theta) & \text{for} \quad -\pi \leqslant \theta \leqslant -\frac{2}{3}\pi \\ \dfrac{-1}{1.6}(0.5) & \text{for} \quad -\frac{2}{3}\pi \leqslant \theta \leqslant 0, \end{cases} \tag{37}$$

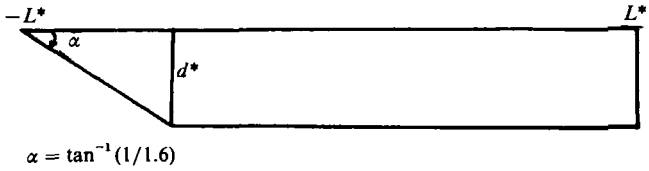

FIGURE 2. Rectangular box with a triangular extension in front.

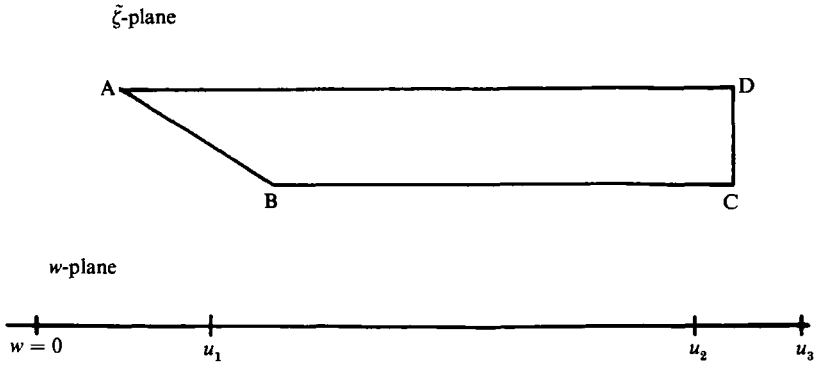

FIGURE 3. Schwarz–Christoffel mapping of a body in the $\tilde{\zeta}$-plane onto the real axis in the w-plane.

with
$$a_n = f_n = \frac{2}{\pi}\int_{-\pi}^{0} f(\theta)\sin n\theta \,\mathrm{d}\theta. \tag{38}$$

The double-body solution can be worked out using a Schwarz–Christoffel transformation. Map the body in the $\tilde{\zeta} = \tilde{x} + \mathrm{i}\tilde{z}$ plane onto the real axis in the w-plane (figure 3) so that the vertices of the body A, B, C, D are mapped onto the points $w = 0, u_1, u_2, u_3$ respectively. Then for $\tilde{G} = \tilde{\phi} + \mathrm{i}\tilde{\psi} = w = u + \mathrm{i}v$,

$$\frac{\mathrm{d}\tilde{G}}{\mathrm{d}\tilde{\zeta}} = \tilde{\phi}_{\tilde{x}} - \mathrm{i}\tilde{\phi}_{\tilde{z}} = \frac{\mathrm{d}\tilde{G}}{\mathrm{d}w}\frac{\mathrm{d}w}{\mathrm{d}\tilde{\zeta}} = \frac{\mathrm{d}w}{\mathrm{d}\tilde{\zeta}} \tag{39}$$

for
$$\frac{\mathrm{d}w}{\mathrm{d}\tilde{\zeta}} = \frac{w^{\alpha/\pi}}{(w-u_1)^{\alpha/\pi}}\frac{(w-u_3)^{\frac{1}{2}}}{(w-u_2)^{\frac{1}{2}}} \tag{40}$$

and
$$\tilde{\zeta} = -A + \int_{s=0}^{w}\left(\frac{s-u_1}{s}\right)^{\alpha/\pi}\left(\frac{s-u_2}{s-u_3}\right)^{\frac{1}{2}}\mathrm{d}s. \tag{41}$$

The points u_1, u_2 and u_3 must be shown so that (41) is satisfied when $\tilde{\zeta}$ is located at the vertices of the body B, C, D and w is located at u_1, u_2, u_3, respectively.

The free-surface solution, $\xi = \epsilon\eta$, for the linear problem and $\xi = F_d^2\tilde{\eta}$, for the double-body problem are plotted in figure 4 where the distance, height and Froude number are scaled according to the draught of the body. The triangular bow is located at $x = -1.6$ in order to match with the experimental measurements presented in figure 6 (*a–d*). Note that the linear solution has a square-root singularity near the body's leading edge while the double-body solution is bounded. Upstream from just a few draught lengths out from the bow, the two solutions are remarkably similar. This is a somewhat surprising result since they arise from very different perturbation expansions and since the downstream solutions are very different. For

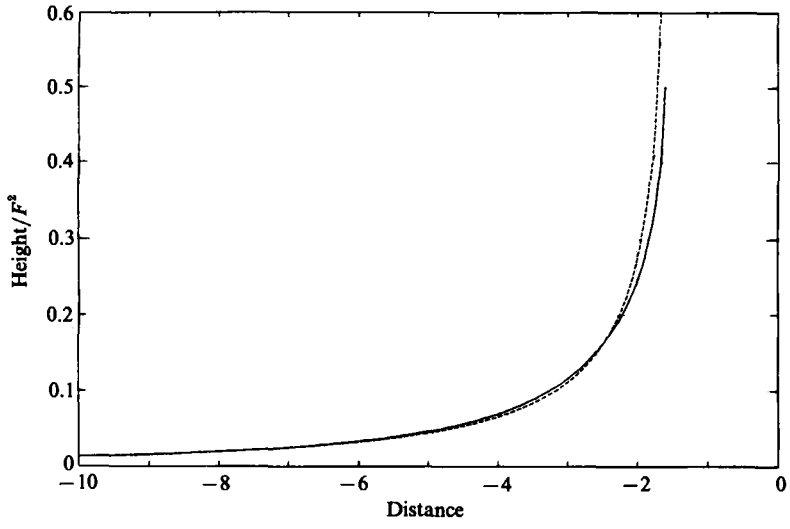

FIGURE 4. Free-surface height for the linear theory (– – – –) and double-body (——) theory past a box with a triangular extension in front.

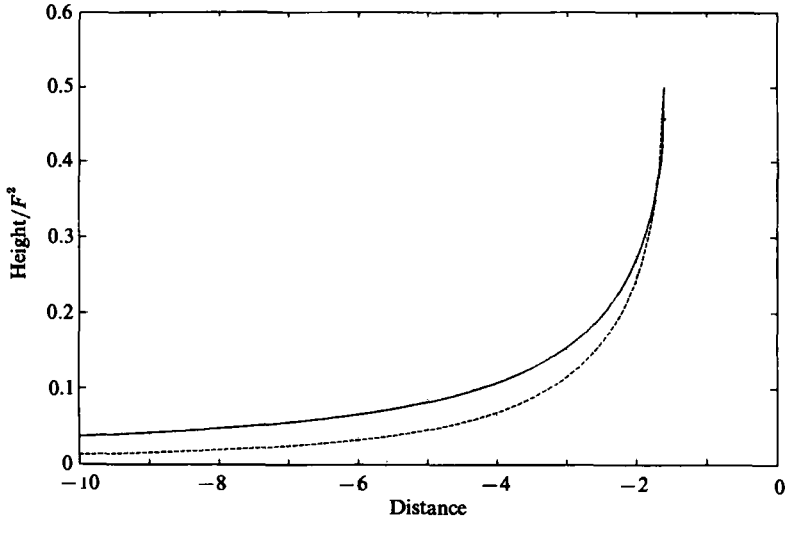

FIGURE 5. Upstream double-body solution for a finite box (– – – –) and a semi-infinite box (——) with the same triangular extension in front.

reference the upstream double-body height for the finite box of figure 2 and a semi-infinite box with the same triangular extension in front are plotted in figure 5.

5. Comparison with experimental results

Measured wave heights are plotted in figure 6(*a–d*) for typical experimental runs along with the double-body solution for flow past a semi-infinite box with a triangular extension in front, for four values of F_d. Note that the vertical axis is greatly stretched relative to the horizontal axis. Wave heights are plotted for the rectangular box up to its bow at $x = 0$ while the double-body measurements extend upstream from the triangular extension at x approximately equal to -1.4 to -1.6

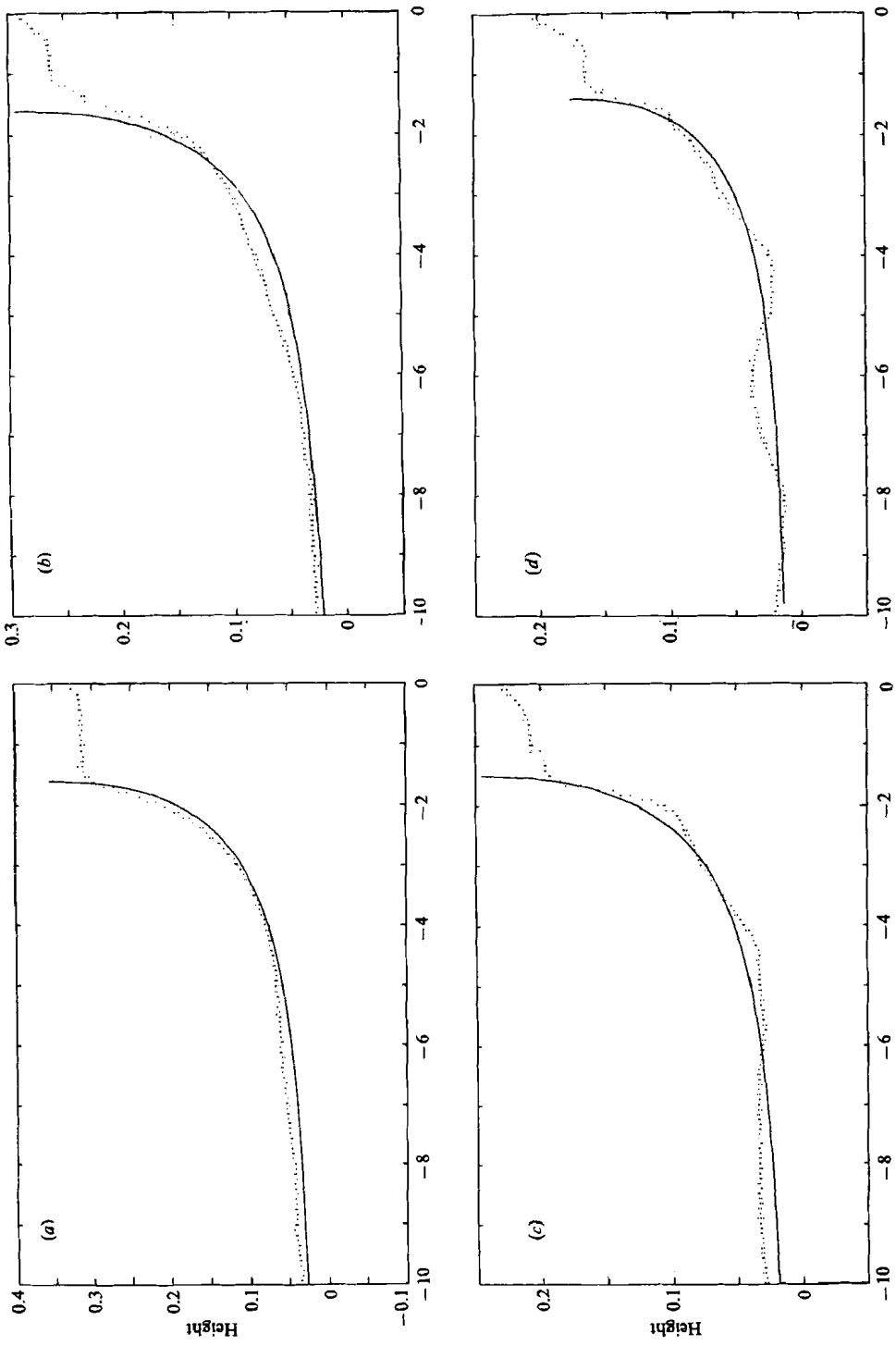

FIGURE 6. (*a*) Measured free-surface height (.....) and theoretical double-body height (——) for (*a*) $F_d^2 = 0.71$, (*b*) 0.58, (*c*) 0.49, and (*d*) 0.35.

draught lengths. Notice that the free surface rises relatively smoothly from upstream and then forms a plateau above the vortical flow region between $x = -1.4$ to -1.6 up to the bow of the rectangular box at $x = 0$. The potential flow separates away from the free surface near the beginning of the plateau region approximately where the free-surface slope becomes discontinuous. Unsteady waves emanate from the bow of the box. At the higher Froude numbers, these waves dissipate relatively quickly in the plateau region while the lower-Froude-number runs show these waves propagating upstream. The flow is turbulent off the body's stern, which in effect extends the length of the body behind. Thus, the theoretical double-body solution past a semi-infinite body is compared to the experimental observations. Although the experimental flow structure is more complicated than the theoretical double-body flow, the two upstream solutions agree fairly well away from the region of strong viscous influence near the plateau.

6. Conclusions

This paper derives a simple asymptotic solution for the linear problem of low-Froude-number two-dimensional flow past a shallow-draught object. The free-surface height is of order ϵF_L^2 in front of the body but has free waves of order ϵF_L behind the body. Upstream and away from the leading edge, $\phi_x \gg \phi_z$ along the surface and the surface height depends on the Froude number to leading order only as a scale factor. This behaviour upstream but away from a body's leading edge where viscous effects are expected to be important is the same as that of double-body flow. Thus, while it is generally accepted that double-body flow accurately models the upstream behaviour of low-Froude-number flow, we now see that the low-Froude-number limit of linear theory (based on a small-draught approximation) behaves in the same way as double-body flow (away from the body's leading edge) yet the linear solution predicts waves downstream. The simple case of flow past a box with a triangular extension in front is worked out as an example. Experimental results of the upstream flow past a box are also presented. Although the experimental flow has a more complicated structure than the linear or double-body flow, the free surface is very similar to the theoretical flow past a semi-infinite box with a triangular extension in front from a few draught lengths out.

REFERENCES

COLE, S. L. 1988 A simple example from flat ship theory. *J. Fluid Mech.* **189**, 301–310.

COLE, S. L. & STRAYER, T. D. 1991 *Mathematical Approaches in Hydrodynamics*, pp. 335–348.

JONES, R. T. 1990 *Wing Theory*. Princeton University Press.

KELDYSH, M. V. 1939 Remarks on some motions of heavy fluids. *Tech. Note Tsentr. Aero-Gidrodin. Inst.* 52.

SEDOV, L. I. 1965 *Two-dimensional Problems in Hydrodynamics and Aerodynamics*, pp. 238–269. Interscience.